Effects of Polypropylene Glycol 400 (PPG400) on the Micellization and Gelation of Pluronic F127

ARTICLE *in* MACROMOLECULES · OCTOBER 2015

Impact Factor: 5.8 · DOI: 10.1021/acs.macromol.5b01655

Macromolecules

Article

pubs.acs.org/Macromolecules

Effects of Polypropylene Glycol 400 (PPG400) on the Micellization and Gelation of Pluronic F127

Carolina Moura de Lima,[†] Sônia M. C. Siqueira,[‡] Antonia F. V. de Amorim,[‡] Kamilla B. S. Costa,[†] Débora H. A. de Brito,[†] Maria E. N. P. Ribeiro,[†] Nadja M. P. S. Ricardo,[†] Chiraphon Chaibunditc,[§] Stephen G. Yeates,[∥] and Nágila M. P. S. Ricardo*[,†]

[†]Department of Organic and Inorganic Chemistry, Polymer Laboratory, Federal University of Ceará, CX 12200 Fortaleza, Brazil

[‡]State University of Ceará, CEP 60740-903, Fortaleza, Ceará, Brazil

[§]Department of Materials Science and Technology, Faculty of Science, Prince of Songkla University, Hat Yai, Songkhla 90112, Thailand

[∥]School of Chemistry, University of Manchester, Manchester M13 9PL, U.K.

Supporting Information

ABSTRACT: In dilute aqueous solution unimers of Pluronic F127 associate to form micelles. In more concentrated solution, micelles pack to form high-modulus gels. Our interest is the effect of addition of 10−30 wt % low molecular weight PPG400 on the micellization and gelation of solutions of F127. DLS was used to determine the apparent size of the micelles ($r_{h,app}$). The critical micelle concentration (cmc) using the dye solubilization method of F127 in PPG400 solutions was studied. Visual observation was carried out to detect gel formation in concentrated solutions and the onset of clouding and turbidity, as the temperature was raised. Oscillatory rheometry was used to confirm the formation of high-modulus gels and provide values of elastic moduli (G'_{max}) over a wide temperature range. SAXS was used to determine gel structure. Our results for the hydrophobic adduct PPG400 were compared with literature values for the hydrophilic adduct PEG6000.

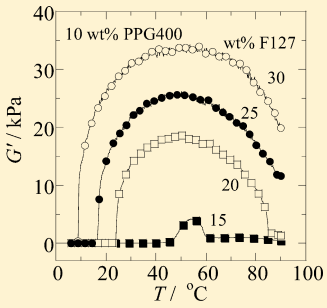

1. INTRODUCTION

Triblock Pluronic copolymers of poly(ethylene oxide) and poly(propylene oxide) are available across a range of compositions.[1] It is convenient to use the notation $E_mP_nE_m$, where E = oxyethylene, OCH_2CH_2, P = oxypropylene, $OCH_2CH(CH)_3$, and subscripts m and n denote number-average block lengths in repeat units. Moderately concentrated aqueous solutions of Pluronic F127 (nominal formula $E_{98}P_{67}E_{98}$) form hard micellar gels at ambient tempearture, and such gels were introduced for treating burns as long ago as 1972.[2] The properties of such gels have been studied across the concentration range 15−50 wt % and at temperatures above 5 °C,[3,4] and small-angle X-ray scattering (SAXS) has been used to identify cubic packing of micelles in the gels.[5,6]

The micellization of copolymer F127 in aqueous solvents modified by the addition of cosolvents has been considered in a recent report by Alexandridis and co-workers.[7] The cosolvents considered in their work ranged from ethanol to propylene carbonate and triacetin, and emphasis was placed on the critical conditions for micelle formation as reflected in the critical micelle concentration (cmc). In the past few years we have also considered the possibility of modifying solutions of F127 but with particular emphasis on the effect of additives on micellar gels formed in relatively concentrated systems. In particular, we have considered the gelation of aqueous solutions of F127 with added ionic surfactant SDS,[8] ethanol,[9] cell-culture media,[10] and water-soluble polymers poly(vinylpyrrolidone) and poly(ethylene oxide).[11] Here we report an extension of our study to the formation of micellar gels in aqueous solutions of F127 containing 10−30 wt % PPG400, a more hydrophobic additive that we have used before. Our interest in the F127/PPG 400/water system arose because it could be used as a structure directing agent in the synthesis of mesoporous materials. Recent publications[12−14] have indicated advantages in expansion of mesoporous structure using polypropylene glycol (PPG3000) as a swelling agent. TEOS was used as the silica source, and F127 was used as the template.

The critical micelle concentration (cmc) of nonionic octaethylene glycol monododecyl ethers ($C_{12}E_8$) and methyl-capped nonionic surfactants (C_8E_4OMe and $C_{10}E_4OMe$) in water, water/ethylene glycol (EG), and water/propylene glycol (PG) has been studied using the tensiometry in refs 15 and 16, respectively. The surface tension results show a strong dependence on the solvent quality. Small-angle neutron scattering (SAN) has been used to study the aggregation properties of octaethylene oxide mono-*n*-alkyl ethers ($C_{12}E_8$, $C_{14}E_8$, and $C_{16}E_8$) in water, water/EG, and water/PG.[17]

In the work critical micelle concentrations were obtained by measuring absorption intensities from solubilized 1,6-diphenyl-1,3,5-hexatriene (DPH) as a function of copolymer concen-

Received: July 24, 2015
Revised: October 1, 2015
Published: October 21, 2015

DOI: 10.1021/acs.macromol.5b01655
Macromolecules 2015, 48, 7978−7982

tration. Dynamic light scattering (DLS) from dilute copolymer solutions was used to determine the hydrodynamic radii of the micelles. Gel boundaries were determined by tube inversion (TI) and were checked by oscillatory shear rheometry, with the elastic moduli of selected gels measured as a function of temperature, range 5−80 °C, and small-angle X-ray scattering (SAXS) was used to check hard gel structure. We note that in our previous work[9−11] all the additives provided optically clear aqueous solutions over the temperature range considered (10−85 °C), whereas 10−30 wt % solutions of PPG400 in water clouded at temperatures in excess of 48−53 °C (see Figure S1, Supporting Information). Opportunity is taken to compare results obtained for F127 and PPG400 with those obtained for F127 and PEG6000.

2. MATERIALS AND METHODS

2.1. Materials. Triblock copolymer F127, a product of BASF Corp. purchased from Sigma, was used as received. The value of the number-average molar mass supplied with the sample was 12 500 g mol^{-1}. A value of the ratio of weight to number-average molar mass, M_w/M_n = 1.20, was determined by gel permeation chromatography using *N*,*N*-dimethylacetamide at 70 °C as solvent and the method described previously.[18] Polypropylene glycol, PPG400, of molecular weight of 400 g mol^{-1} was purchased from Fluka and used as received.

2.2. Dye Solubilization Method. The cmc was determined by measuring the change in the absorption intensity of 1,6-diphenyl-1,3,5-hexatriene (DPH) added to solutions of F127 plus PPG400 following the method described by Chattopadhyay and London[19] and Alexandridis et al.[20] The copolymers were dissolved in Milli-Q water allowing 24 h for complete dissolution and then diluted to concentrations within the range 10 μg dm^{-3}−10 g dm^{-3}. DPH was dissolved in methanol and added to the copolymer solutions so that the final copolymer solution contained 1% (v/v) methanol and 0.004 mM DPH. The absorption measurements were performed using a Hitachi U-2000 UV−vis spectrometer with the solution temperatures maintained at 30 ± 0.2 °C. The absorption peak at 356 nm was recorded and its intensity plotted as a function of copolymer concentration. The point of sharp change in the absorption intensity corresponded to the cmc of the copolymer.

2.3. Dynamic Light Scattering (DLS). Solutions were clarified by filtering through Millipore Millex filters (Triton free, 0.1 μm) directly into cleaned scattering cells. In certain experiments, the most concentrated solution was filtered and subsequently diluted with filtered solvent. DLS measurements were made by means of a Brookhaven BI200S instrument using vertically polarized incident light of wavelength 488 nm supplied by an argon-ion laser operated at 500 mW or less. A Brookhaven BI9000AT digital correlator was used to acquire data. The duration of an experiment was 10 min, and each experiment was repeated two or more times. Scattered light intensity was measured at an angle of 90° to the incident beam.

The correlation functions from DLS were analyzed by the constrained regularized CONTIN method[21] to obtain distributions of decay rates (Γ) and hence distributions of apparent mutual diffusion coefficient [$D_{app} = \Gamma/q^2$, $q = (4\pi n/\lambda)\sin(\theta/2)$, n = refractive index of the solvent, and λ = wavelength] and ultimately of apparent hydrodynamic radius ($r_{h,app}$, radius of the hydrodynamically equivalent hard sphere corresponding to D_{app}) via the Stokes−Einstein equation

$$r_{h,app} = kT/(6\pi\eta D_{app}) \quad (1)$$

where k is the Boltzmann constant and η is taken to be the viscosity of the water at temperature T. In practice, intensities $I(\Gamma)$ delivered by the CONTIN program at logarithmically spaced values of the decay rate were transformed to $I(\log\Gamma) = I(\Gamma)\Gamma$ to obtain intensity distributions of $\log(\Gamma)$ and hence of $\log(r_{h,app})$. Normalization of $I(\log r_{h,app})$ gave the intensity fraction distributions presented in section 3.1. Values of $r_{h,app}$ averaged over the intensity distribution were also delivered by the program.

2.4. Turbidity and Gelation. Onset temperatures of turbidity and gelation were measured to ±1 °C by enclosing samples of aqueous solutions (0.5 g) in small tubes and observing while heating them slowly (0.1 °C min^{-1}) in a water bath through the temperature range 5−90 °C. Gelation was recognized by immobility of the solution when the tube was inverted at intervals of 1 °C.

2.5. Rheometry. Samples were prepared in small vials and stored for at least 1 week at 5 °C to reach equilibrium. A strain-controlled ARES rheometer (TA Instruments) with cone-and-plate geometry (diameter 50 mm, angle 0.04 rad) and with Peltier control of plate temperature (±0.1 °C) was used in oscillatory-shear mode at frequency f = 1 Hz to determine elastic (G') and loss (G'') moduli as the samples were heated from 5 °C at 1 °C min^{-1}. The strain amplitude was held at a low value (A = 0.005), thus ensuring that measurements of G' and G'' were in the linear viscoelastic region. A solvent trap maintained a solvent-saturated atmosphere around the cell, but evaporation of solvent from the edge of the cone-and-plate cell limited measurements to temperatures below 80−85 °C. Each experiment was repeated twice.

2.6. Small-Angle X-ray Scattering. Experiments for 30 wt % F127 in 10, 20, and 30 wt % PPG400 were performed on OMIC laboratories, Manchester University, UK. The instrument was a HECUS X-ray Systems GMBH GRAZ, S3-Micro and Xenocs Cu K-alpha Microfocus X-ray Source. The wavelength was 1.44 Å, and the sample−detector distance was 275 mm. The data were collected using a Pilatus 100 K detector. The wavenumber scale ($q = 4\pi \sin\theta/\lambda$, scattering angle = 2θ, wavelength λ = 1.033 Å) was calibrated with silver behenate.

Experiment was done at 30 °C for 1000 s. Samples were clamped between polyester sheets before introduction into the vacuum system. Temperature control was achieved via a water chiller from Xenocs. Scattering curves were monitored over a q-range from 0.12 to 0.02 Å^{-1}, and the 2D images were converted to 1D using ASA3 software.

3. RESULTS AND DISCUSSION

3.1. Hydrodynamic Radii. Intensity fraction distributions of $\log(r_{h,app})$ are shown in Figure 1. The broad peaks centered

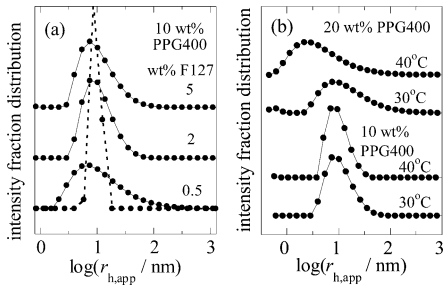

Figure 1. Dynamic light scattering. Intensity fraction distributions of the logarithm of apparent hydrodynamic radius for solutions of F127: (a) 10 wt % PPG400 at 30 °C and the concentrations of F127 indicated and (b) 2 wt % F127 in 10 and 20 wt % PPG400 at 30 and 40 °C. The dashed curve in (a) is for 2 wt % F127 in water.

at 10 nm shown in Figure 1a are those obtained for dilute aqueous solutions of F127 (0.5, 2, and 5 wt %) containing 10 wt % PPG400. The contrasting sharp peak (dashed curve) is that for 2 wt % F127 in water alone taken from ref 4—the areas of all peaks are normalized. Figure 1b shows corresponding intensity distributions for 2 wt % F127 and 10 and 20 wt % PPG400 at 30 and 40 °C. Compared with solutions containing 10 wt % PPG400, the intensity distributions for 20 wt % PPG400 at 30 °C are broader, and those for solutions at 40 °C peak at lower values, $r_{h,app} \sim 3$ nm. Intrinsic values of r_h obtained by extrapolation of a range of average values of $1/r_{h,app}$ to zero F127 concentration are listed in Table 1 and serve to

DOI: 10.1021/acs.macromol.5b01655
Macromolecules 2015, 48, 7978−7982

Table 1. Intrinsic Hydrodynamic Radii of Micelles of F127 in Water Alone and in Aqueous Solutions of PPG400

wt % PPG400	T/°C	r_h/nm[a]
0[b]	40	12.5
10	30	9.4
	40	9.7
20	30	9.9
	40	7.1

[a]Estimated uncertainty: $r_h \pm 1$ nm. [b]Obtained from ref 4.

confirm the low value of r_h at the high PPG400 concentration and high temperature. Corresponding plots for F127 in 30 wt % PPG400 were scattered, and values of $r_{h,app}$ could not be determined.

3.2. Critical Micelle Concentration. Plots of absorption intensity at 356 nm from 1,6-diphenyl-1,3,5-hexatriene (DPH) added to aqueous solutions of F127 plus PPG400 and held at T = 30 °C are shown in Figure 2.

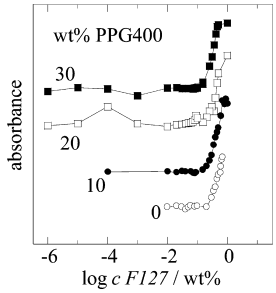

Figure 2. Absorbance intensity from DPH for F127 in (○) water, (●) 10 wt % PPG400, (□) 20 wt % PPG400, and (■) 30 wt % PPG400. T = 30 °C.

Values of the cmc determined as the concentration at which the absorption intensity increased rapidly are listed in Table 2. The cmc of F127 is following the order 30 wt % PPG400 < 20 wt % PPG 400 < 10 wt % PPG400 < water. Addition of PPG400 reduces the cmc, i.e., favors micelle formation.

Table 2. Cmc of F127 in Water Alone and in Solutions Containing 10, 20, and 30 wt % PPG400 (T = 30 °C)

wt % PPG400	cmc/wt %
0	0.26
10	0.21
20	0.19
30	0.15

3.3. Phase Diagram: Tube Inversion. Figure 3 shows phase diagrams for solutions of F127 dissolved in water alone and in aqueous solutions of 10, 20, and 30 wt % PPG400. The boundaries in Figure 3 were defined by observation in the tube inversion experiments supplemented by rheology. The critical concentration of F127 for gel formation in water, 15 wt %, was essentially unchanged on adding 10 or 20 wt % PPG400, though the corresponding temperature increased from 46 °C (water) to 55 °C (10 wt % PPG400) and further to 63 °C (20 wt % PPG400). However, the critical concentration for gel formation increased markedly to 22 wt % F127 on adding 30 wt % PPG400, while the corresponding temperature fell to

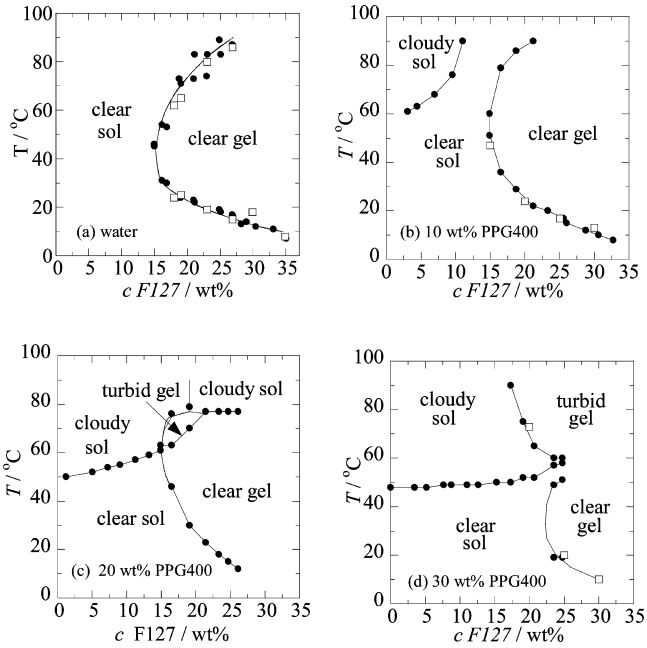

Figure 3. Phase diagrams of F127 in (a) water, (b) 10 wt % PPG400, (c) 20 wt % PPG400, and (d) 30 wt % PPG400. (a) is adapted from ref 4. The data points refer to (●) the tube inversion method and to (□) rheology.

30 °C. Selected high and low temperature limits of gel formation extracted from Figure 3 are summarized in Figure S2.

As noted in section 1, and as illustrated in Figure S1, 10−30 wt % solutions of PPG400 in water clouded at temperatures in excess of 50−55 °C. For solutions containing 10 wt % PPG400 (see Figure 3b), the clouding temperature increased on gradual addition of F127, eventually to reach a value in excess of 90 °C at 11 wt % copolymer. At higher F127 concentrations the system remained clear, presumably with PPG400 solubilized in the high-T range in the cores of the micelles. As seen in Figure 3c, solutions containing 20 wt % PPG400 clouded across the F127 concentration range at temperatures increasing from 50 °C (1 wt % F127) to 79 °C (30 wt % F127), i.e., consistent with solubilization being restricted to temperatures below 80 °C in this system. With 30 wt % PPG400 (Figure 3d) solutions and gels clouded across the F127 concentration range on heating to temperatures in the range 50−60 °C, much as recorded for solutions in water alone, i.e., an indication that 30 wt % PPG400 in micellar solutions of F127 approached the solubilization capacity of the system.

3.4. Rheology. Figure 4 shows temperature scans of elastic modulus for 15, 20, 25, and 30 wt % F127 in water and in 10, 20, and 30 wt % PPG400. Compared with solutions of PPG400 in water, values of the maxima in the plots of elastic modulus against temperature (G'_{max}) increase marginally with addition of 10 wt % PPG400 but then decrease as the concentration of PPG400 is increased to 20 wt % and further to 30 wt %. The transition from clear gel to turbid gel seen in Figure 3d for the solution with 30 wt % PPG400 and 30 wt % F127 is clearly defined in the rheology scan at $T \sim 65$ °C, G' = 5−6 kPa, with a more complex transition for 25 wt % F127 at a lower temperature, T = 40−50 °C and G' = 2−4 kPa. Otherwise, the data points from rheology shown in Figure 3 refer to temperatures at which G' had values less than 2 kPa.

3.5. Gel Structure. The SAXS profiles of 30 wt % F127 in 10, 20, and 30 wt % PPG400 at 30 °C are shown in the

DOI: 10.1021/acs.macromol.5b01655
Macromolecules 2015, 48, 7978−7982

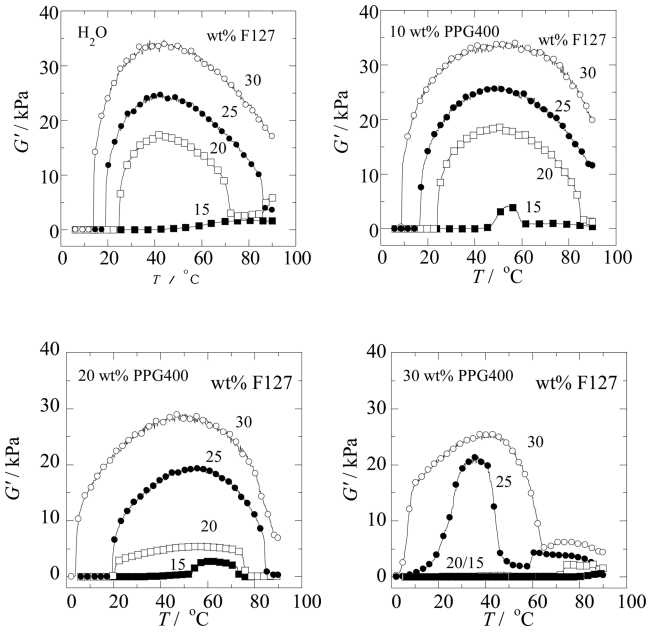

Figure 4. Temperature dependence of elastic modulus (G') for solutions of copolymer F127 in water alone and in 10, 20, and 30 wt % aqueous solutions of PPG400: f = 1 Hz and A = 0.005. The concentrations of F127 are as indicated.

Supporting Information. The values of q at the first-order reflection (q^*), the d-spacing (calculated as $d = 2\pi/q^*$), and the gel structure are listed in Table 3. Relative to the main peak, the values of q for the two minor peaks detected are in ratio 1, $\sqrt{2}$, $\sqrt{3}$, characteristic of the bcc structure. The structure of the gel of 30 wt % F127 in water is known to be fcc.[4,11]

Table 3. Assignment of SAXS Reflections: Peak Position (q^*) and d-Spacing for 30 wt % F127

			peak position	
wt % PPG400	T/°C	structure	q^*/Å^{-1}	d/Å
0[a]	30	fcc	0.042	150
10	30	bcc	0.0435	144
20	30	bcc	0.0445	141
30	30	bcc	0.0467	134

[a]Taken from ref 11.

3.6. Comparison with the Micellization and Gelation of F127 in Solutions Containing PEG6000. The different effects of addition of hydrophobic and hydrophilic oligomers on the gelation of aqueous solutions of F127, including PPG400 and PEG6000, were investigated some time ago by Malmsten and Lindman.[22] Here we take the opportunity to combine a more recent study[11] of the effect of addition of hydrophilic PEG6000 with results for PPG400 taken from the present work. Representative results are illustrated in Figure 5. In view of the relatively narrow concentration range available for PEG6000 the comparison is restricted to 20 wt % PPG400.

As pointed out by Malmsten and Lindman,[22] the polarity of the solvent is decreased by addition of either PEG6000 or PPG400, and micellization and gelation might be limited on that account. The significant increase in hydrodynamic radius (r_h) seen in Figure 5a for micelles of F127 in aqueous solutions containing hydrophilic PEG6000 is consistent with it being compatible with the E-blocks of the micelle corona, so leading

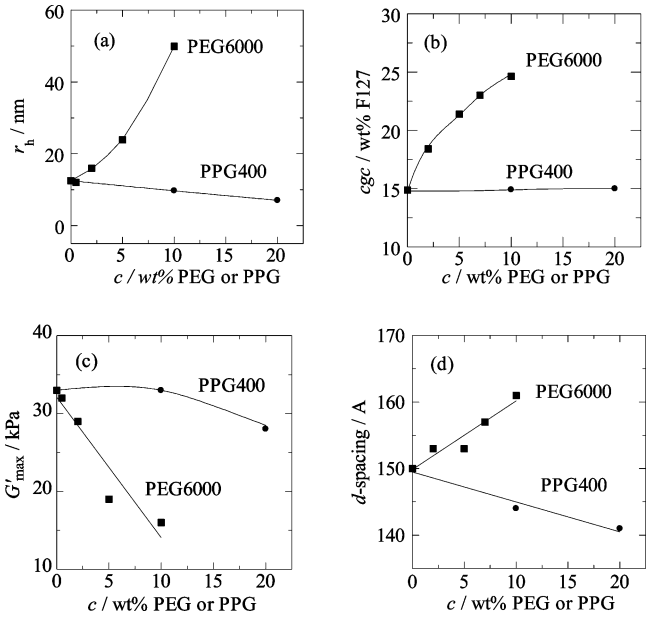

Figure 5. F127 dissolved in aqueous solutions of (■) PEG6000 and (●) PPG400. (a) Intrinsic hydrodyanmic radii (r_h) of micelles in dilute solution, T = 40 °C: (b) critical concentrations of F127 for gelation; (c) maximum values of the elastic modulus (G'_{max}) of 30 wt % F127 gels; (d) d-spacing in 30 wt % F127 gels, T = 30 °C. The curves are intended to lead the eye through the data points. The results for PEG6000 are taken from ref 11.

to an increase in micelle size and the formation of micelle clusters, as reported for related systems.[23,24] No such effect is possible for hydrophobic PPG400, and any reduction in micelle size attributable to change in polarity of the solvent is modified by removal of PPG400 from the solvent phase by solubilization in the micelle core.

The same considerations apply to the values of the critical concentration for gel formation (cgc) recorded in Figure 5b. The increase in cgc on addition of PEG6000 to solutions of F127 is due to the decrease in polarity of the solvent which limits micelle formation, the more so as the PEG concentration is raised from 1 to 10 wt %. In contrast, and as noted above, solubilization of PPG400 in the micelle cores counteracts any reduction in solvent polarity, and the cgc is constant at 15 wt % across the range 0−20 wt % PPG400 (Figure 5b). Equally the fall in the strength of the gel, as measured by the elastic modulus G' and seen (Figure 5c) for F127 solutions containing PEG6000 in the range 1−10 wt %, reflects limited micellization in that system, in contrast to the almost constant and high values of G' recorded for gels of F127 in PPG400 solutions.

As seen in Figure 5d, the effect of adding PEG6000 is to increase the d-spacing of the gel, and that of adding PPG400 is to decrease the d-spacing. This would be expected; comparison with Figure 5a shows that the d-spacings in the gel are closely related to the radii of micelles determined for dilute solution.

4. CONCLUDING REMARKS

The micellization of Pluronic F127 in 10 and 20 wt % PPG400 solution was studied using dynamic light scattering. The intensity fraction distributions of $\log(r_{h,app})$ of F127 in PPG400 solutions are broader than that for F127 in water. The intrinsic hydrodynamic radii (r_h) of micelle of F127 in PPG400 solution decrease as wt % PPG400 increase up to 20 wt %. The cmc of F127 in 10, 20, and 30 wt % PPG400 solution determined

DOI: 10.1021/acs.macromol.5b01655
Macromolecules 2015, 48, 7978−7982

using the dye solubilization method decreases as wt % PPG400 increases.

The cloudy solution temperature of 10−50 wt % PPG400 solutions alone was studied (see Figure S1). The solution cloudy temperature of F127 in 10 and 20 wt % PPG400 increases compared to 10 and 20 wt % PPG400 solution. The cloudy solution temperature of F127 in 30 wt % PPG400 is similar to 30 wt % PPG400 solution. The gel boundary of hard gel increases as wt % PPG400 increases.

The rheology of 15, 20, 25, and 30 wt % F127 in water and 10, 20, and 30 wt % PPG400 solutions was studied. The G'_{max} of hard gel decreases as wt % PPG400 increases to 20−30 wt %. The SAXS profiles obtained for high concentration gel (30 wt % F127) are present in Figure S3. The *d*-spacing of 30 wt % F127 in PPG400 decreases as PPG400 concentration increases. The gel structure of 30 wt % F127 in PPG400 shows the bcc structure compared to the fcc structure for 30 wt % F127 in aqueous solution.

The micellization and gelation of F127 in 10−20 wt % PPG400 have been compared with those in 2−10 wt % PEG6000.[11] The micelle radii of F127 in PPG400 slowly decrease, whereas those increase in PEG6000 solutuion. The cgc of F127 in PPG400 solution is constant, whereas that in PEG6000 solution significantly increases.[11,22] The G'_{max} of 30 wt % F127 in PEG 6000 significantly decreases compared with the slight decrease in PPG400. The *d*-spacing of 30 wt % F127 in PEG6000 increases whereas that slightly decreases in PPG400.

■ ASSOCIATED CONTENT

Supporting Information

The Supporting Information is available free of charge on the ACS Publications website at DOI: 10.1021/acs.macromol.5b01655

Figures S1−S3 and Table S1 (PDF)

■ AUTHOR INFORMATION

Corresponding Author

*E-mail naricard@ufc.br; Tel +55 85 33669142; Fax +55 85 33669978 (N.M.P.S.R.).

Notes

The authors declare no competing financial interest.

■ ACKNOWLEDGMENTS

This work was supported by CNPq, the Brazilian Research Council (Processo 304392/2013-8) and INCT (N.M.P.S.R.), CAPES (C.M.L.) the PSU Research fund, Thailand (C.C.), and the Organic Materials Innovation Centre, University of Manchester. The authors thank Dr. Colin Booth for his constant help.

■ REFERENCES

(1) Alexandridis, P.; Hatton, T. A. *Colloids Surf., A* **1995**, *96*, 1−46.
(2) Schmolka, I. R. *J. Biomed. Mater. Res.* **1972**, *6*, 571−582.
(3) Wanka, G.; Hoffmann, H.; Ulbricht, W. *Colloid Polym. Sci.* **1990**, *268*, 101−117.
(4) Chaibundit, C.; Ricardo, N. M. P. S.; Costa, F.; de, M. L. L.; Yeates, S. G.; Booth, C. *Langmuir* **2007**, *23*, 9229−9236.
(5) Mortensen, K.; Talmon, Y. *Macromolecules* **1995**, *28*, 8829−8834.
(6) Ivanova, R.; Lindman, B.; Alexandridis, P. *Langmuir* **2000**, *16*, 9058−9069.
(7) Sarkar, B.; Ravi, V.; Alexandridis, P. *J. Colloid Interface Sci.* **2013**, *390*, 137−146.
(8) Chaibundit, C.; Ricardo, N. M. P. S.; Ricardo, N. M. P. S.; O'Driscoll, B. M. D.; Hamley, I. W.; Yeates, S. G.; Booth, C. *Langmuir* **2009**, *25*, 13776−13783.
(9) Chaibundit, C.; Ricardo, N. M. P. S.; Ricardo, N. M. P. S.; Muryn, C. A.; Madec, M.-B.; Yeates, S. G.; Booth, C. *J. Colloid Interface Sci.* **2010**, *351*, 190−196.
(10) Zhang, H.; Ding, J. *J. Biomater. Sci., Polym. Ed.* **2010**, *21*, 253−269.
(11) Ricardo, N. M. P. S.; Ricardo, N. M. P. S.; Costa, F.; de, M. L. L.; Bezerra, F. W. A.; Chaibundit, C.; Hermida-Merino, D.; Greenland, B. W.; Burattini, S.; Hamley, I. W.; Nixon, S. K.; Yeates, S. G. *J. Colloid Interface Sci.* **2012**, *368* (1), 336−341.
(12) Sörensen, M. H.; Corkery, R. W.; Pedersen, J. S.; Resenholm, J.; Alberius, P. C. *Microporous Mesoporous Mater.* **2008**, *113*, 1.
(13) Sörensen, M. H.; Valle-Delgado, J. J.; Corkery, R. W.; Rutland, M. W.; Alberius, P. C. *Langmuir* **2008**, *24* (14), 7024−7030.
(14) Sörensen, M. H.; Zhu, J.; Corkery, R. W.; Hayward, R. C.; Alberius, P.C. A. *Microporous Mesoporous Mater.* **2009**, *120*, 359−367.
(15) Seguin, C.; Eastoe, J.; Rogers, S.; Hollamby, M.; Dalgliesh, R. M. *Langmuir* **2006**, *22* (26), 11187−11192.
(16) Seguin, C.; Eastoe, J.; Heenan, R. K.; Grillo, I. *J. Colloid Interface Sci.* **2007**, *315* (2), 714−720.
(17) Seguin, C.; Eastoe, J.; Clapperton, R.; Heenan, R. K.; Grillo, I. *Colloids Surf., A* **2006**, *282*−*283*, 134−142.
(18) Chaibundit, C.; Mai, S.-M.; Heatley, F.; Booth, C. *Langmuir* **2000**, *16*, 9645.
(19) Chattopadhyay, A.; London, E. *Anal. Biochem.* **1984**, *139* (2), 408−412.
(20) Alexandridis, P.; Holzwarth, J. F.; Hatton, T. A. *Macromolecules* **1994**, *27* (9), 2414−2425.
(21) Provencher, S. W. *Makromol. Chem.* **1979**, *180* (1), 201−209.
(22) Malmsten, M.; Lindman, B. *Macromolecules* **1993**, *26* (6), 1282−1286.
(23) Feitosa, E.; Brown, W.; Wang, K.; Barreleiro, P. C. A. *Macromolecules* **2002**, *35* (1), 201−207.
(24) Ge, L.; Zhang, X.; Guo, R. *Polymer* **2007**, *48* (9), 2681−2691.

DOI: 10.1021/acs.macromol.5b01655
Macromolecules 2015, 48, 7978−7982